KSABC
The Korean Society for Applied Biological Chemistry

ARTICLE   **Open Access**

Anti-neuroinflammatory effects of the KIOM-patented *Polygonum multiflorum* maximized root tuber against LPS-stimulated BV2 Cells

Tae Woo Oh[1,3]* , Yeongjun Ban[2] and Youngmin Kang[2,3]*

Abstract

The main pathological mechanism of neurodegeneration is neuroinflammation. It is known that the persistent neuroinflammatory response is harmful by causing secondary nerve tissue damage. Meanwhile, *P. multiflorum* is a traditional oriental medicinal herb. It has been used as a hematopoietic agent and is used to treat a variety of diseases and conditions. The aim of the present study was to compare the anti-inflammatory efficacy between the commonly available *P. multiflorum* (C1) and the KIOM-patented in vitro-propagated *P. multiflorum* (K1), which had higher content of active ingredients and biomass, using culture and cultivation conditions of LPS-induced neuroinflammation. After stimulation with LPS and treatment with C1 and K1 in mouse microglial BV-2 cells, nitric oxide (NO) production, pro-inflammatory cytokine secretion, inducible NO synthase (iNOS) expression, MAPK phosphorylation and transcription factor activity were assessed. We examined the antioxidant effect using DPPH and production of nitric oxide (NO). C1 and K1 suppressed the expression of iNOS and COX-2 and the production of pro-inflammatory cytokines. Furthermore, we determined the levels of inflammatory mediators, such as interleukin (IL)-1β, IL-6, tumor necrosis factor (TNF)-α and mitogen-activated protein kinases and IκBα via Western blotting to understand the regulating mechanisms. Additionally, C1 and K1 also inhibited the activation of p38 and nuclear factor-kappa B (NF-κB) in LPS-stimulated BV2 cells. In all experimental results, excellent anti-neuroinflammatory effects were confirmed at a lower dose in K1 than in C1, which is believed to be due to the increased biomass. Therefore, K1 is expected to be more effective than C1 and can be applied more broadly in the development of prevention and treatment of various inflammatory-mediated neurodegenerative diseases.

Keywords KIOM-patented *Polygonum multiflorum*, Lipopolysaccharide, Microglia, Neuroinflammation, Neuroprotection

*Correspondence:
Tae Woo Oh
taewoo2080@kiom.re.kr
Youngmin Kang
ymkang@kiom.re.kr
[1] Korean Medicine (KM)-Application Center, Korea Institute of Oriental Medicine (KIOM), 70 Cheomdan-ro, Dong-gu, Daegu 41062, Republic of Korea
[2] Herbal Medicine Resources Research Center, Korea Institute of Oriental Medicine (KIOM), 111 Geonjae-ro, Naju-si, Jeollanam-do 58245, Republic of Korea
[3] University of Science and Technology (UST), Korean Convergence Medicine Major KIOM, 1672 Yuseongdae-ro, Yuseong-gu, Daejeon 34054, Republic of Korea

Introduction

As life expectancy increases, the social and economic costs of chronic neurodegenerative diseases, such as Alzheimer's disease (AD), Parkinson's disease (PD), and Lou Gehrig's disease, increase significantly [1]. Neurodegenerative diseases are characterized by progressive dysfunction and cell death in specific parts of the nervous system and are known to be caused by genetic, environmental, and aging-related endogenous factors [2]. Neuroinflammation is a common pathological mechanism of neurodegeneration; when it becomes chronic, it is known to be harmful by causing nervous

Oh *et al. Applied Biological Chemistry* (2024) 67:71

Page 2 of 11

tissue damage secondary to continuous microglia activity. Microglia that are distributed throughout the brain are actual central nervous system (CNS) macrophages that produce inflammatory cytokines upon activation by substances, such as lipopolysaccharide (LPS), β amyloid, thrombin, and interferon (IFN) γ [3, 4]. It induces the secretion and gene expression of proinflammatory cytokines, inducible nitric oxide synthase (iNOS) and cyclooxygenase-2 (COX-2). Excessive activity of the microglial cells that continue in this cycle results in the secretion of mediators that disturb the homeostasis of the immune system, causing the development and progression of multiple sclerosis, AD, PD, and autoimmune-related neurodegenerative diseases [5]. Therefore, understanding the innate immune system dysregulation caused by microglial hyperactivation and controlling the inflammatory mediators secreted by abnormally activated microglia might be an approach to slow the progression of chronic inflammatory diseases or treat damage.

The root tuber of *Polygonum multiflorum* Thunb., which belongs to the *Polygonaceae* family, is a medicinal herb that has been traditionally used in Traditional Korean Medicine (TKM) as a blood-tonifying medicine [6]. The TKM book Dong-Eui-Bo-gam stated that in addition to its function as a hematopoietic drug, it is used for antiaging and to strengthen cognitive function and bones. Moreover, it has been reported to have a strong protective effect on hippocampal neurons [7]. The processed form of *P. multiflorum* is used, because it is more effective than the raw product. Previously, we developed an optimum in vitro propagation protocol to produce high-quality *P. multiflorum* seedlings and rootstocks [8]. In that research, we aimed to reduce the toxicity and increase the beneficial effects of medicinal herbs through processing, which is one of the core theories of TKM. To optimize the use of *P. multiflorum* in TKM, the Korea Institute of Oriental Medicine (KIOM) patented our submission (no: 10-2019-0120751, September 30, 2019) as a standard protocol for rapid in vitro production of seedlings and expanded roots. Subsequently, the potential impacts of the KIOM-manufactured *P. multiflorum* on bone formation with osteoblast-like Saos-2 cells and bone resorption using bone marrow-derived macrophage cells were shown [9]. Moreover, the *P. multiflorum* processing technique was reported to be appropriate and enabled confirmation of the content of active compounds through exposure to different adjunct materials [10, 11].

In this present study, we compared the commercially available *P. multiflorum* and the KIOM-patented and in vitro-propagated *P. multiflorum* in terms of superior effects on neuroinflammation and the mechanisms.

Materials and methods
Materials and reagents
We purchased 2 kg of dried roots of the commercially available *P. multiflorum* from Jirisan Hasuo Farming Co. (Sancheong, Republic of Korea); this was authenticated by the Herbarium of KIOM as commercial raw *P. multiflorum* (C1). Raw *P. multiflorum* dried root tubers (2 kg) that were produced by the KIOM-patented protocol (patent no. 10–1777833) were provided by KIOM and prepared as K1. The details of the preparation were followed, as previously reported [9, 11]. Dulbecco's modified Eagle's medium (DMEM) was purchased from Welgne Inc. (Gyeongsan, Koea). Fetal bovine serum (FBS) and penicillin/streptomycin antibiotics were obtained from Hyclone (Logan, UT, USA). All cell culture dishes and plates were acquired from SPL Life Sciences (Pocheon, Republic of Korea). LPS, glutamate, 3-(4,5-dimethylthiazol-2-yl)-2,5-diphenyltetrazolium bromide (MTT), dimethyl sulfoxide (DMSO) and Griess reagent were obtained from Sigma–Aldrich (St. Louis, MO, USA). Enzyme-linked immunosorbent assay (ELISA) kits were obtained from R&D Systems (Minneapolis, Minnesota, 88 USA). Various primary antibodies and horseradish peroxidase (HRP)-conjugated secondary antibodies for Western blot analysis were purchased from Cell Signaling Technology, Inc. (Boston, 89 MA, USA).

Sample preparation
C1, which is a wild type of the propagated *P. multiflorum* seed, served as the control group and was produced by Chamdeulae Bio (Sancheong-gun, Gyeongsangnam-do, Republic Korea). K1 was prepared by in vitro propagation of *P. multiflorum* in ethnomedicine, in order to maximize root tuber production for use. Dried *P. multiflorum* (10 g) was placed in 100 mL of distilled water for 2 h at 20 °C and was extracted by centrifuge at 200 rpm. The extracts of each sample were passed through filter paper (ADVANTEC, 110 mm, Toyo Robni kaisha, Japan); concentrated using an evaporator (EYELA, Tokyo Rikakikai, Japan); then dissolved in 70% ethanol. The supernatant was separated using a centrifugal separator to set the final concentrations of the analytical samples to 10 and 20 mg/mL. The reagents used for extraction and dissolution were of HPLC grade (J.T. Baker Inc., Phillipsburg, NJ, USA), and a 0.2-μm membrane filter (PALL Corporation, Ann Arbor, MI, USA) was used.

DPPH radical scavenging activity
The 2,2-diphenyl-1-picrylhydrazyl (DPPH) solution (0.20 mM) was dissolved in methanol, before preparing samples (C1 and K1) at various concentrations (0.0625, 0.125, 0.25, 0.5, 1, 2, and 4 mg/mL). Thereafter, 150 μL of the DPPH solution was mixed with 50 μL of

Oh *et al. Applied Biological Chemistry*   (2024) 67:71

Page 3 of 11

each sample concentration. After 15 min of incubation in a dark room, decrease in the absorbance of the solution was measured at 517 nm. Inhibitory activity against DPPH was expressed as percentage inhibition (%) in the assay system using the following formula:

$$\text{DPPH radical scavenging activity (\%)} = (A\ \text{control} - A\ \text{sample})/A\ \text{control} \times 100$$

where A sample was the absorbance of the test sample and A control was the absorbance of the control.

Cell culture and maintenance

The microglial cell line BV2 was purchased from Professor Kyoungho Suk of Kyungpook National University (Daegu, Republic of Korea) and grown in DMEM, which contained 10% FBS and 1% antibiotics. The cell culture was maintained in a humidified incubator (37 °C, 95% air, and 5% CO_2) during cultivation. The culture medium was renewed every 2 days, and cells were grown to 80–85% confluence for the experiments. The cells were treated with 100 ng/mL of LPS in the presence of C1 or K1. For cellular applications, LPS and glutamate were dissolved in distilled water.

Cytotoxicity investigation using MTT assay

To confirm the cytotoxicity of C1 and K1 and set the experimental conditions, the BV2 cells were cultured in a 24-well plate for 24 h to reach 2×10^5 cells/well. Thereafter, various concentrations of C1 and K1 were treated for 1 h, then 0.1 µg/mL of LPS was added for 24 h before culture. After 24 h, the medium was removed, and 0.5 mg/mL of 3-(4,5-dimethylthazol-2-yl-2,5-teterazolium bromide (MTT, Sigma Aldrich, St. Louis, MO, USA)) was added; this mixture was incubated for 2 h for reduction. After inducing the reaction, formazan crystals were dissolved in dimethyl sulfoxide solution, and the 540-nm absorbance was measured using a microplate reader (Molecular Devices, Sunnyvale, CA, USA) under conditions without LPS and drug treatment. The cell survival rates (%) of the treatment groups were calculated, based on the control group culture.

Measurement of nitric oxide (NO)

The concentration of nitric oxide (NO) produced by the LPS-activated BV2 cells was detected using the Griess reagent, which recognized the NO_2^- in the cell culture. For this purpose, the BV2 cells (2×10^5 cells/well) were cultured in a 24-well plate for 24 h, then treated with various concentrations of C1 or K1 for 1 h before treatment with LPS (0.1 µg/mL). After culturing for 24 h, the cell culture medium was collected and reacted with an equal amount of Griess reagent at room temperature. Afterward, the absorbance of the reaction solution was measured at 540 nm using a microplate reader.

Prostaglandin E2 measurement

To measure the amount of prostaglandin E2 (PGE2) produced by the LPS-stimulated BV2 cells, the cell cultures prepared under the same conditions were collected and tested using a PGE2 enzyme immunoassay kit (Cayman Chemical Company, Ann Arbor, MI, USA). The PGE2 concentration (pg/mL) in the cell culture was calculated and converted, based on the concentration of the standard solution.

Total RNA extraction, DNA synthesis, and RT-qPCR

The BV2 cells (1×10^6 cells/well) were distributed in a 6-well plate, pretreated with C1 or K1 at concentrations of 100 and 200 µg/mL for 1 h, treated with LPS (0.1 µg/mL), and cultured for 6 h. The liquid was removed. Total RNA was extracted using the easy-BLUE™ RNA extraction kit (iNtRON Biotech), according to the manufacturer's protocol, and cDNA was synthesized from the purified RNA and reverse transcribed using AccuPower® CycleScript RT PreMix (Bioneer). In all processes, the fold change in gene expression was corrected for the amount of RNA, which was simultaneously measured using the 2-ΔΔCT method. The base sequence of each primer is shown in Table 1.

Table 1 Specific primer sequences for PCR

Target	Primer sequences		Accession numbers
TNF-α	Forward	5′-ATGAGCACAGAAAGCATG ATC-3′	D84199.2
	Reverse	5′-TACAGGCTTGTCACTCGA ATT-3′	
IL-6	Forward	5′-AGTTGCCTTCTTGGGACT GA-3′	NM_031168.2
	Reverse	5′-CAGAATTGCCATTGCACA AC-3′	
IL-1β	Forward	5′-GGGCCTCAAAGGAAAGAA TC-3′	NM_008361.4
	Reverse	5′-TACCAGTTGGGGAACTCT GC-3′	
GAPDH	Forward	5′-CAGCCTCGTCCCGTAGAC A-3′	NM_008084
	Reverse	5′-CGCTCCTGGAAGATGGTG AT-3′	

Oh *et al. Applied Biological Chemistry* (2024) 67:71

Page 4 of 11

ELISA for cytokine determination

To investigate the inhibitory effects of C1 and K1 on inflammatory cytokine production, the amounts of TNF-α, IL-1β, and IL-6 produced by the BV2 cells the cell culture medium were measured using enzyme-linked immunosorbent assay (ELISA) kit (R&D Systems, Minneapolis, MN, USA), according to the manufacturer's protocol. For this purpose, 50 µL of $1 \times$ assay diluent solution was added, then 50 µL of the cell culture medium or the standard protein for each cytokine was added and reacted at room temperature for 2 h. This mixture was washed in buffer three times, followed by addition of the antibody for detection and reaction at room temperature for 2 h. After washing in buffer 3 times, 100 µL of the color reagent solution was added; this mixture was reacted in the dark at room temperature for 30 min, followed by addition of 100 µL of reaction stop solution. The degree of reaction on the plate was measured by absorbance in a microplate reader. The concentration of each cytokine secreted by the BV2 cells was calculated based on the standard quantitative curve of the standard solution.

Western blot analysis

To investigate the effects of C1 and K1 on the protein expressions of iNOS, COX-2, mitogen-activated protein kinases (MAPK), IκB, and NF-κB, the BV2 cells were distributed on 6-cm dishes at 5×10^6 cells/dish, treated with C1 or K1, washed with ice-cold PBS, then washed in lysis buffer (1-M Tris–HCl, 5-M NaCl); cells were lysed using Triton X-100, which is a protease inhibitor cocktail. The resulting solution was centrifuged at 14,000 rpm for 15 min, the supernatant was recovered, the amount of protein was quantified using BSA standard solution, and 30 µg of protein was electrophoresed using a 9–12% polyacrylamide gel. The gel was separated and transferred to a nitrocellulose membrane, followed by blocking of the proteins with 5% BSA at room temperature for 1 h. The antibodies against each target protein were added and reacted at 4 °C overnight, then washed 3 times with PBS-T solution. Afterward, antiIgG-conjugated HRP antibody was added and reacted at room temperature for 1 h. The mixture was washed again for three times with PBS-T, followed by the addition of enhanced chemiluminescence Western blotting detection reagents (SuperSignal, Thermo Scientific, Rockford, IL, USA). The expression levels were measured using the ChemiDocTM Touch Imaging System (Bio-Rad, Hercules, CA, USA).

Immunofluorescence

The BV2 cells were seeded on 4-well chambered coverslips at 3×10^3 cells/well for cell culture (Ibidi, Gräfelfing, Germany) and cultured in a CO_2 incubator. The BV2 cells were treated with 250 µg/mL of C1 or K1 for 1 h, followed by LPS (0.1 µg/mL) for 20 min. Afterward, the cells were fixed with 4% formaldehyde and cold 100% methanol, treated with blocking buffer containing 5% FBS, and placed in 0.3% Triton X-100 and p65. For visualization, the cells were treated with goat antirabbit IgG (H&L) conjugated with Alexa Fluor ® 488 antibody. For p65 staining of the cytoplasm (red) and nucleus (blue), the cells were mounted in VECTASHIELD Antifade Mounting Medium (Vector Laboratories, Burlingame, CA, USA) containing 4',6-diamidino-2-phenylindole (Vector Laboratories, Burlingame, CA, USA). The translocation of p65 was observed through a fluorescence microscope, and images were recorded with LAS X (Leica Microsystems, Wetzlar, Hessen, Germany).

Quantitative analysis by HPLC

The analysis experiment was conducted quantitatively using an HPLC system (HITACHI L-2000 series HPLC system, Hitachi, Japan). A 250×4.6-mm, 5-µm column was used (Agilent Zorbax Eclipse Plus C18) at a temperature of 25 °C, and the sample temperature was 25 °C. The mobile phase solvent A was 0.1% acetic acid, and solvent B was 100% acetonitrile. The flow rate of the mobile phase was 1.0 mL/min, and the sample injection volume was 10 µL. The total analysis time was set to 80 min. Gradient elution for solvent B was as follows: 0–5 min for 10%, 5–45 min for 40%, 45–51 min for 50%, 51–58 min for 80%, 58–67 min for 98%, and 67–80 min for 98%. The ultraviolet spectrum was measured at a wavelength of 288 nm after scanning from 190 to 400 nm. The compounds for the calibration curve were THSG, emodin, and physcion (Sigma Aldrich Co., Inc. FLUKA, TraceSELECT, USA), using concentrations of 7.8125, 15.625, 31.25, 62.5, 125, and 250 µg/mL. The HPLC quantitative analysis was triplicated and compared with the average content.

Statistical analysis

All the results are presented as mean ± SD (or SEM). One-way analysis of variance using GraphPad Prism version 5.03 for Windows (GraphPad Software Inc., San Diego, CA, USA) was performed for multi-group comparisons. T-tests were applied to analyze the significance of the variations among the groups.

Results

Effects of C1 and K1 on DPPH radical scavenging activity

To compare the antioxidant activities between C1 and K1, a radical scavenging assay was performed using DPPH. C1 and K1 at 10–1000 µg/mL exhibited significant DPPH free radical scavenging activity in a
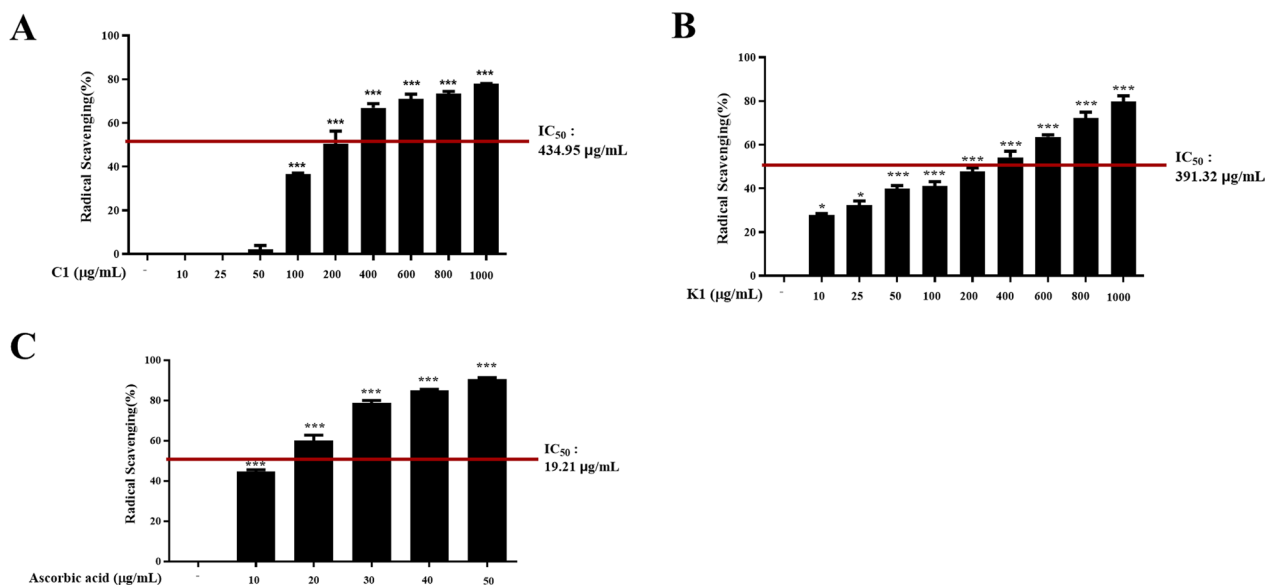
Fig. 1 DPPH radical scavenging of C1 (**A**), K1 (**B**) DPPH radical scavenging of Ascorbic acid (**C**). Values are shown as mean ± SD of three independent experiments. Experimental data are considered statistically significant at values. *p < 0.05 and ***p < 0.001 in comparison with the CTL group

concentration-dependent manner (Fig. 1). The concentration required to inhibit DPPH radicals by 50% was 434.95 μg/mL for C1 and 391.32 μg/mL for K1 (p < 0.001).

Effect of C1 and K1 on microglial cell viability

The BV2 cell line takes advantage of the characteristics of microglia and has been widely used as a replacement for primary microglia in brain inflammation experiments. To determine the cytotoxicity of C1 and K1 and the maximum concentration for this activity, the BV2 cells were treated with various concentrations of C1 and K1, treated with LPS in culture for 24 h, then subjected to MTT assay to measure cell survival rate. The MTT assay confirmed the absence of cytotoxicity after treating the cells with C1 or K1 at a concentration of 1.0 mg/mL (Fig. 2A, B). Based on these results, the experiment was conducted at a C1 or K1 concentration of ≤ 0.25 mg/mL, excluding 0.5 mg/mL.

Effect of inhibitory on NO and PGE2 production by C1 and K1 in LPS-activated BV2 microglial cells

The BV2 cells were treated with 0.1 μg/mL of LPS to induce NO production, then with C1 and K1 to confirm the inhibitory effects on the production of NO, which is an inflammatory mediator. The NO concentration in the cell culture medium was measured using the Griess reaction method. In addition, the ability of C1 and K1 to effectively inhibit PGE2, which is another inflammatory mediator produced by BV2 cells, was measured using ELISA. As shown in Fig. 2C, the level of NO was low in the BV2 cells that were not given LPS but was

significantly increased after LPS treatment, confirming LPS activation of the BV2 cells. Decreased production of LPS-induced NO was confirmed after pretreatment with C1 at 250 μg/mL and with K1 at both 100 and 250 μg/mL in a concentration-dependent manner. The concentration of PGE2 in the BV2 cells in the culture medium was low without LPS stimulation but was confirmed to be significantly increased after LPS treatment (Fig. 2D). Treatment with C1 or K1 at concentrations of 25, 50, 100, and 250 μg/mL, respectively, greatly reduced PGE2 production in a concentration-dependent manner, the activity of K1 was found to be superior to that of C1.

Inhibitory effects of C1 and K1 on inflammatory cytokine expression in LPS-activated BV2 microglial cells

Based on the significantly suppressed LPS-induced NO and PGE2 production after C1 and K1 treatment, we investigated the effects on the production of proinflammatory cytokines. Among various cytokines, TNF-α, IL-1β, and IL-6 were investigated for the effects of C1 and K1 using RT-PCR to measure mRNA expression and ELISA to measure protein expression. As shown in Fig. 3A–C, treatment with LPS (0.1 μg/mL) increased the mRNA expression of all inflammatory cytokines. After C1 and K1 treatment, the mRNA expressions of *IL-1β* and *IL-6* were significantly suppressed in a concentration-dependent manner. On the other hand, the mRNA expression of *TNF-α* did not appear to be significantly affected by C1 but was significantly inhibited by K1 at a high concentration (250 μg/mL). On ELISA (Fig. 3D–F), the concentrations of TNF-α, IL-1β, and IL-6 were very

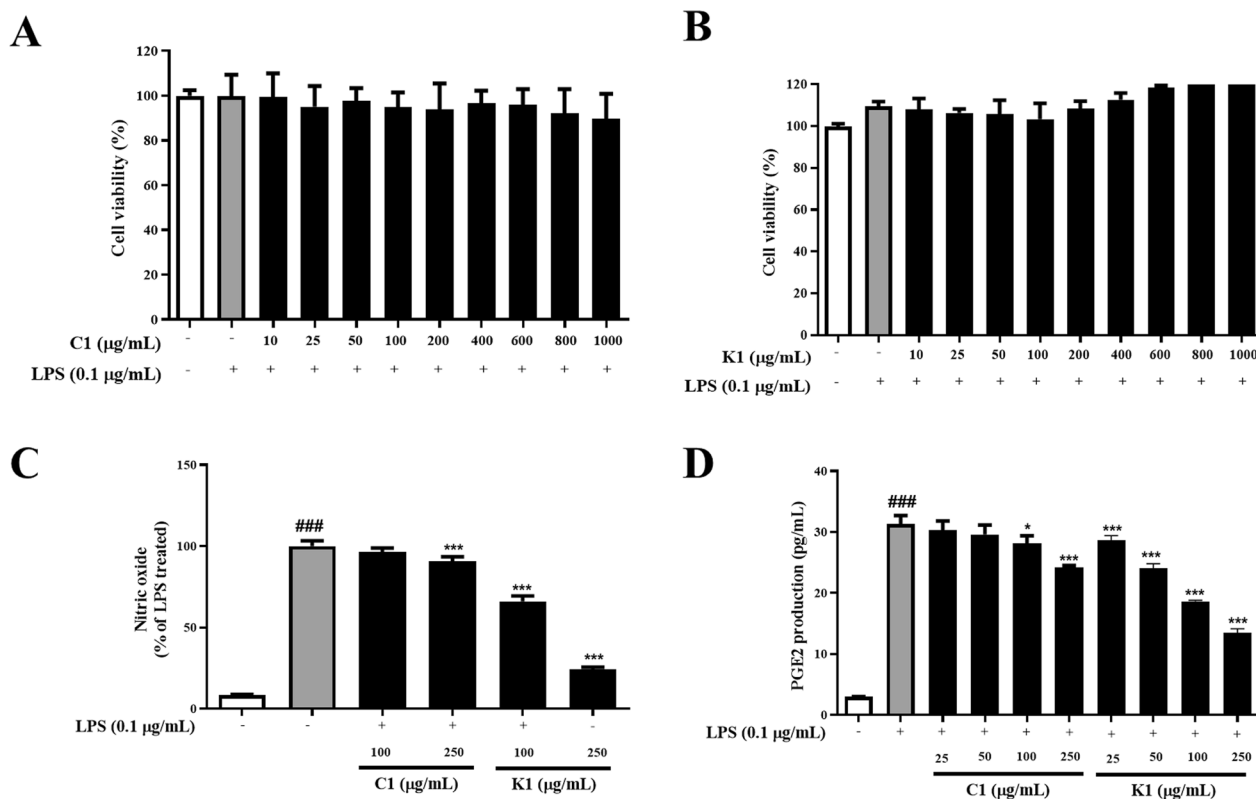Oh *et al. Applied Biological Chemistry*   (2024) 67:71

Page 6 of 11

Fig. 2 The cell viability was determined by MTT assay (**A**, **B**), NO (**C**) and PGE2 production (**D**) in BV2 cells. BV2 cells were seed in 96-well plate at a density of 1X10^5 cells/well. After overnight growth, the cells were treated with C1, K1 and LPS (0.1 μg/mL) for another 24 h. After 24 h incubation period, MTT assay were measured. Values are shown as mean ± SD of three independent experiments. Experimental data are considered statistically significant at values. $^{###}$ $p < 0.001$, significant difference compared to control; $^*p < 0.05$ and $^{***}p < 0.001$ in comparison with the LPS group

low in the BV2 cells cultured under normal conditions but significantly increased to 4.3 pg/mL, 7.1 pg/mL, and 288.7 pg/mL, respectively, after treatment with LPS alone. The LPS-induced production of TNF-α, IL1-β, and IL-6 was suppressed in a concentration-dependent manner by K1 but not by C1, similar to the effects seen on inflammatory cytokine gene expression.

Effects of C1 and K1 on iNOS, COX-2, and MAPK activities in LPS-activated BV2 microglial cells

Based on the previously observed significant inhibition of LPS-induced NO and PGE2 production, the effects of C1 and K1 treatment on the expression of iNOS, which is a NO synthase, and COX-2, which is a major enzyme for PGE2 production, were investigated by Western blotting. The expressions of iNOS and COX-2 in the cultured BV2 cells were very low under normal conditions but markedly increased after stimulation with LPS (0.1 μg/mL) (Fig. 4A). After treatment with C1 and K1, the LPS-induced protein expressions of iNOS and COX-2 were significantly suppressed in a

concentration-dependent manner. Similarly, the effects of C1 and K1 on activation of MAPK, which is a representative pathway that controls and inhibits inflammatory responses, were confirmed at the protein level through Western blot (Fig. 4B). Phosphorylation of p38 MAPK, extracellular signal-regulated kinase (ERK), and c-Jun N-terminal kinase (JNK) were all strongly induced in the BV2 cells treated with LPS but were significantly inhibited after C1 and K1 treatment.

Effects of C1 and K1 on NF-κB activation in LPS-activated BV2 microglial cells

We used immunofluorescence staining to compare the intracellular and nuclear distributions and expressions of NF-κB at the genetic and protein levels. First, immunofluorescence staining demonstrated that most of the NF-κB expressed in the BV2 cells cultured under normal conditions (without LPS) were in the cytoplasm; in the LPS-activated BV2 cells, the nuclear expression of the NF-κB p65 subunit increased (Fig. 5A).
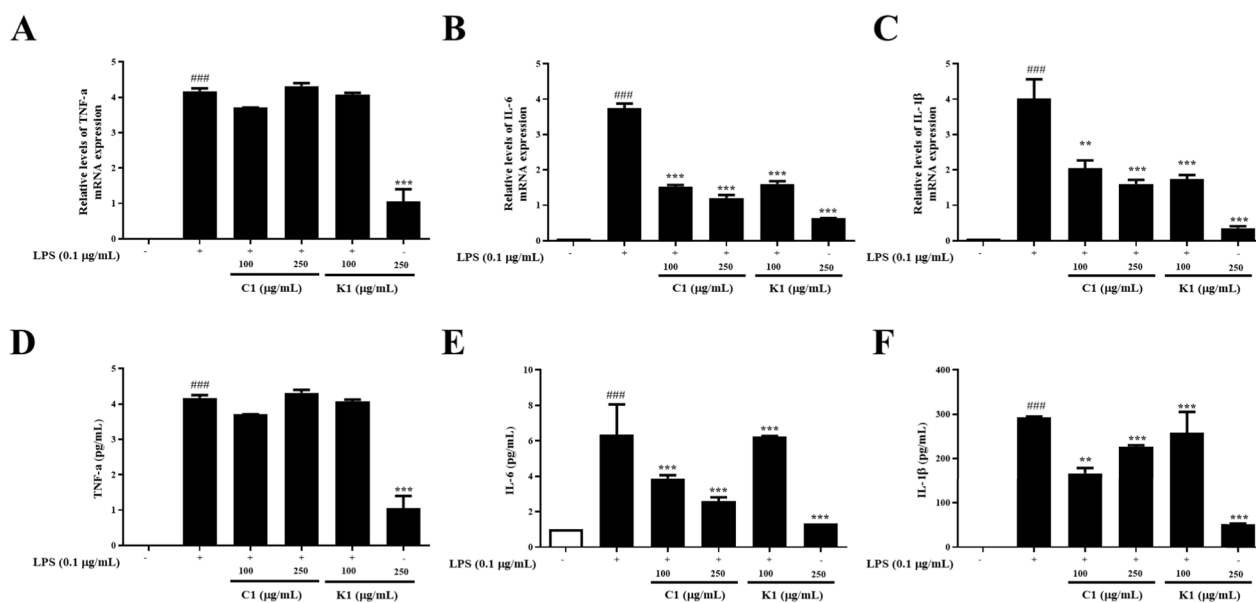
Oh *et al. Applied Biological Chemistry*   (2024) 67:71

Page 7 of 11

Fig. 3 TNF-α (**A**), IL-6 (**B**) and IL-1β (**C**) gene expression (real time-PCR) and inflammatory mediator production such as TNF-α (**D**), IL-6 (**E**) and IL-1β (**F**) in BV2 cells. BV2 cells were seed in 6-well plate at a density of 3X10⁶ cells/well. After overnight growth, the cells were treated with C1, K1and LPS (0.1 μg/mL) for another 24 h. After 24 h incubation period, mRNA levels of TNF-α, IL-6 and IL-1β were measured using real-time qPCR (**A**-**C**). The levels of pro-inflammatory cytokines were quantified by ELISA (**D**-**F**). Values are shown as mean ± SD of three independent experiments. Experimental data are considered statistically significant at values. ### p < 0.001, significant difference compared to control; ***p < 0.001 in comparison with the LPS group
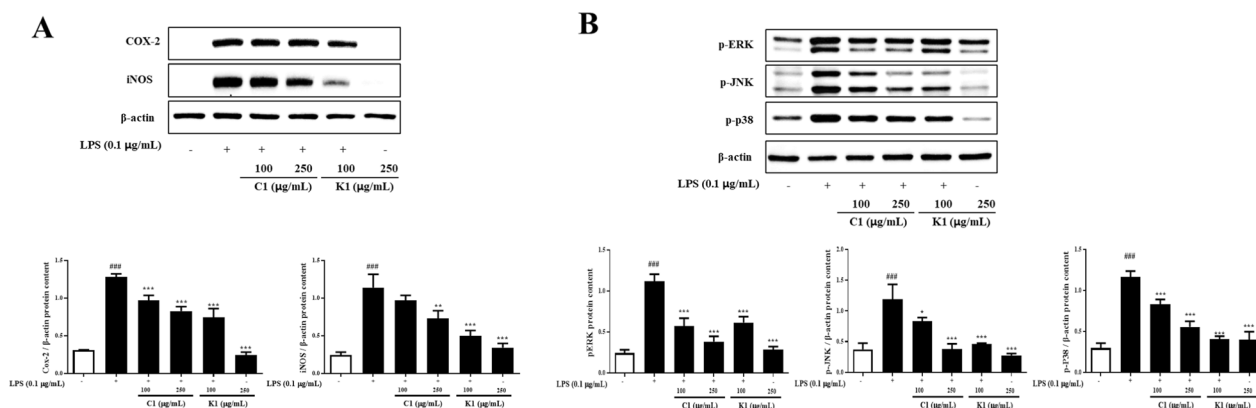

Fig. 4 The effect of C1 and K1 on the LPS-induced expression of iNOS and COX-2 protein (**A**) and MAPK phosphorylation (**B**) in BV2 cells. BV2 cells were seed in 6-well plate at a density of 3X10⁶ cells/well. After 24 h, the cells were pretreated with C1 and K1 for 1 h, and then stimulated with LPS (0.1 μg/mL). The level of expression of iNOS and COX-2 proteins and mitogen-activated protein kinase (MAPK) phosphorylation level of ERK, JNK, p38s determined by Western blot analysis. Values are shown as mean ± SD of three independent experiments. Experimental data are considered statistically significant at values. ### p < 0.001, significant difference compared to control; *p < 0.05,**p < 0.01 and ***p < 0.001 in comparison with the LPS group

Treatment with C1 and K1 significantly suppressed the LPS-induced NF-κB nuclear translocation. After LPS treatment, the expression of the NF-κB p65 subunit was significantly decreased in the cytoplasm and increased in the nucleus (Fig. 5B). On the other hand, LPS treatment decreased the expression of I-κBα in the cytoplasm.

Quantitative analysis by HPLC

The results of the HPLC analysis are shown in Fig. 6. The yield of the extracts for quantitative analysis was 15.5% for C1 and 23.7% for K1. The chromatogram indicated increments of the main compounds of K1, then C1. Quantitative analysis using the calibration curves demonstrated that compared with C1, K1 contained
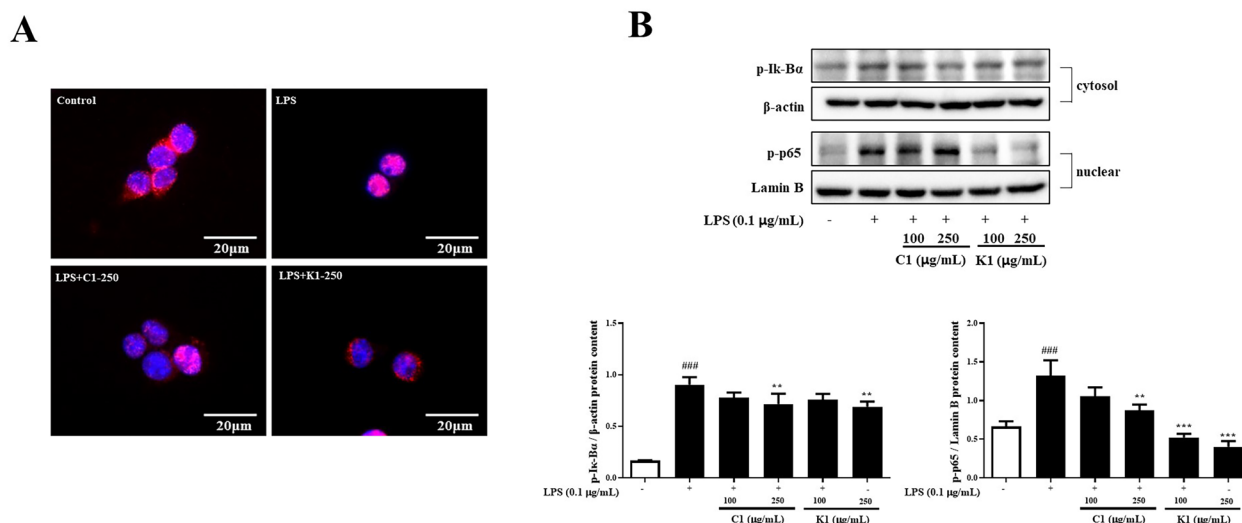
Oh *et al. Applied Biological Chemistry*   (2024) 67:71

Page 8 of 11

Fig. 5 The effect of C1 and K1 on the LPS-induced expression of NF-κB (**A**) and pathway (**B**) in in BV2 cells. BV2 cells were seed in 6-well plate at a density of 3X10^6 cells/well. After 24 h, the cells were pretreated with C1 and K1 for 1 h, and then stimulated with LPS (0.1 μg/mL) for 20 min. After the treatment, Immunofluorescence staining results of p65 in LPS stimulated microglial cells (**A**) and the cytosol and nucleus were prepared of Western blot analysis (**B**). Values are shown as mean ± SD of three independent experiments. Experimental data are considered statistically significant at values. $^{\#\#\#}$ $p < 0.001$, significant difference compared to control; $^{**}p < 0.01$ and $^{***}p < 0.001$ in comparison with the LPS group
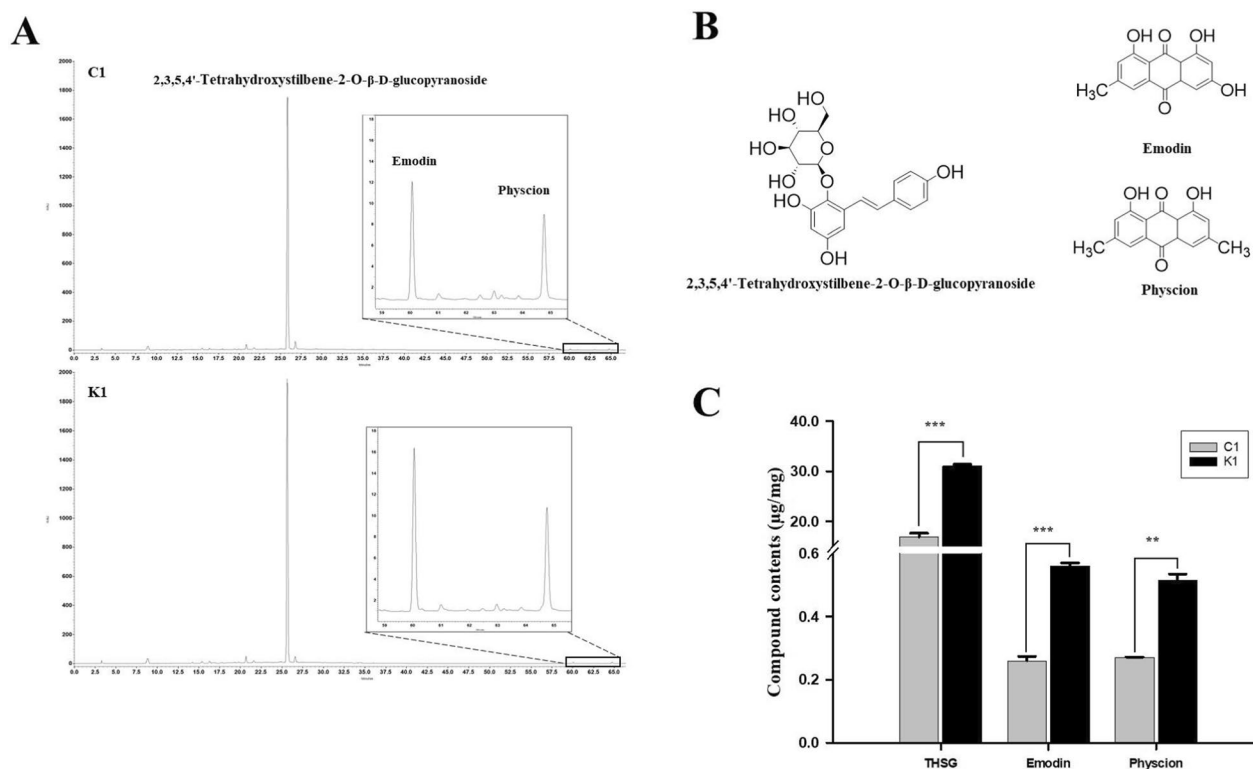

Fig. 6 The HPLC chromatogram of extract C1 and K1 (**A**), main compounds structure (**B**), and comparison of main compound contents (**C**). Dilution concentration for HPLC analysis was 10 mg/mL for 2,3,5,4'-tetrahydroxystilbene-2-O-β-D-glucopyranoside and 20 mg/mL for emodin and physcion. The final contents of main compounds were calculated by applying the extraction yield. Extraction yield was 15.5% for C1 and 23.7% for K1. Values are shown as mean ± SD of three independent experiments. Experimental data are considered statistically significant at values. $^{**}p < 0.01$ and $^{***}p < 0.001$ in comparison with extract C1 and K1

higher concentrations of THSG (30.95 ± 0.46 μg/mg vs. 16.83 ± 0.79 μg/mg), emodin (0.55 ± 0.01 μg/mg vs. 0.26 ± 0.01 μg/mg), and physcion (0.53 ± 0.02 μg/mg vs. 0.27 ± 0.01 μg/mg). As an effect of processing to maximize root tuber production using the optimized standard cultivation [8, 9], K1 was superior to C1 in terms of higher content of THSG by 1.8 times, emodin by 2.16 times, and physcion by 1.8 times.

Discussion

Microglia have the classical function of CNS phagocytic cells, which regulate the initial immune responses; inflammatory cytokines, such as TNF-α, IL-1β, and eicosanoids; and reactive oxygen species (ROS) [12]. Excessive secretion of ROS, NO, and superoxide anion contributes to the development of degenerative diseases. Early neuroinflammation ensues as a protective response in the brain, but excessive inflammatory response can be harmful and actually reduce nerve regeneration, causing neurodegenerative diseases and other neurological disorders [13]. After a single or chronic exposure to disease-related proteins, environmental toxins, cytokines, or nerve damage, microglia, which regulate neuroinflammation, are continuously activated to produce cytokines and ROS, leading to neuroinflammation and gradual loss of nerves (i.e., neurodegenerative disease) [14, 15]. The bacterial endotoxin LPS is a major substance that causes inflammation; activates microglia to produce NO, PGE2, TNF-α, IL-1β, monocyte chemoattractant protein-1, and macrophage inflammatory peptide-1; and leads to excessive secretion of IL-16, IL-18, and macrophage colony-stimulating factor, which act as cytotoxic substances and accelerate the inflammatory response, thereby, contributing to the development of chronic diseases [16–18].

Therefore, the production of inflammatory mediators by activated BV2 cells and the expression of related genes had been recognized as useful for both the treatment of inflammatory diseases and the prevention and treatment of various diseases. In this study, we aimed to compare the antiinflammatory efficacy between the commonly available *P. multiflorum* (C1) and the KIOM-patented in vitro-propagated *P. multiflorum* (K1), which had higher content of active ingredients and biomass, using culture and cultivation conditions of LPS-induced neuroinflammation. We investigated the production of various inflammatory mediators and the changes in the expression of their respective genes within a noncytotoxic range.

DPPH is a water-soluble substance that contains a chemically stabilized free radical. It can be reduced by ascorbic acid, tocopherol, and polyhydroxy aromatic compounds, which result in decolorization of the deep purple color [19]. This method has been widely used to screen for antioxidants in various natural materials. Most of the ROS produced are removed by the defense mechanisms of the body; those that are not removed rapidly react with biological molecules and cause protein denaturation, lipid peroxidation of biological membranes, and DNA damage. The lipid peroxides diffuse into cells or travel through the bloodstream to promote new radical reactions and cause various diseases. In this study, measurement of the DPPH radical scavenging activities found that compared with C1, K1 had superior antioxidant ability at a lower concentration. Moreover, both C1 and K1 showed no cytotoxicity at 1.0 mg/mL.

NO is a type of toxic reactive nitrogen species that has a low molecular weight and is involved in the defense function of the immune system [20, 21]. NO is produced by L-arginine in macrophages through the NO synthesis enzymes, including constitutive NOS and iNOS. iNOS is produced by microglia in response to inflammatory stimuli, such as LPS, TNFα, IFNγ, or IL-1β. Excessive NO secretion in vivo causes cytotoxicity, promotes inflammatory responses, mediates inflammatory responses in the CNS, and is involved in the development of neurodegenerative diseases [22, 23]. Meanwhile, certain prostaglandin families are known to gradually worsen the inflammatory responses. COX, lipoxygenase, or cytochrome P-450 monooxygenase converts arachidonic acid into PGE2, PGD2, PGF2α, PGI2, and thromboxane A2, which are the five major prostaglandins synthesized [24]. Similar to NO, PGE2 is the best-known mediator of the inflammatory response and contributes to the development of various inflammatory diseases [25]. According to the results of this study, C1 and K1 significantly reduced the LPS-activated NO and PGE2 production in the BV2 cells. Moreover, compared with C1, K1 was found to be superior in inhibiting neuroinflammation by significantly reducing the protein expression levels of iNOS and COX-2 in a concentration-dependent manner.

Cytokines play essential roles in immunity, infection, hematopoietic function, tissue recovery, cell growth, and body defense. They are substances that mediate the pathological and physiological responses to various diseases. Activated microglia secrete cytokines, such as IL-1β, IL-6, IL-10, TGF-β, and TNFα, which are expressed at very low levels under normal conditions but are highly expressed under excessive injury and can act as factors that promote inflammation. IL-1β, IL-6, and TNFα are the representative cytokines, which directly or indirectly cause neurodegeneration, damage the neuronal cells in neurodegenerative diseases, and are known to contribute to mortality [26, 27]. In this study, we found that in LPS-activated BV2 cells, both C1 and K1 significantly suppressed the production and gene expressions of IL-1β and IL-6 at the transcriptional level, but only K1 caused a

Oh *et al. Applied Biological Chemistry*   (2024) 67:71

Page 10 of 11

concentration-dependent decrease in the production and gene expression of TNFα. These results suggested the capability of K1 to suppress TNFα production and effectively alleviate inflammation-related brain diseases and symptoms.

The signal transduction process of the MAPK subfamily, which includes ERK, JNK, and p38, induces the synthesis of proinflammatory mediators. The inflammatory response initiated and activated by pathogen infection, which produces LPS, phosphorylates the MAPK molecules and activates transcriptional regulators, such as NF-κB and activator protein-1 to produce free radicals, such as NO and superoxide anion [28, 29]. MAPKs are involved in the production of neuroinflammatory regulators and regulate cell functions, including survival, death, and inflammation [30]. In this study, we confirmed the anti-neuroinflammatory effects of C1 and K1 through effective inhibition of MAPK phosphorylation in LPS-activated BV2 cells. In particular, compared with C1, K1 was confirmed to inhibit p38 MAPK phosphorylation better and in a concentration-dependent manner. Recently, the importance of p38 inhibitors has emerged, based on findings of worsening neurodegenerative diseases secondary to MAPK-mediated neuroinflammation in microglial cells [31]. K1 inhibition of MAPK phosphorylation shows high potential as a treatment for neuroinflammation. Moreover, C1 and K1 were found to inhibit nuclear translocation of the NF-κB p65 subunit. Therefore, C1 and K1 inhibition of MAPK and NF-κB activities seemed to directly affect the inhibition of inflammatory cytokine expression.

In CRS mice, the major active compound THSG has been reported to reduce oxidative stress in the central and peripheral nervous systems and was shown to suppress inflammatory responses, based on the increased expressions of inflammatory factors TNF-α, IL-1β, and IL-6 in the hippocampus and prefrontal cortex [32]. Moreover, THSG was reported to decrease ROS generation and exhibit significant neuroprotective effects against glutamate-induced hippocampal damage [33]. Emodin is another major active compound that has been reported to inhibit neuronal cell death through its antioxidant activity, reduce Aβ deposition and neuroinflammation in APP/PS1 mice, increase the expression of antioxidant enzymes, and protect mitochondrial function, thereby, inhibiting neuronal cell death [34]. Compared with C1, K1, which was processed through vegetative propagation under improved culture and cultivation conditions, was confirmed on HPLC to have higher content and biomass of the three main active ingredients 2,3,5,4'-tetrahydroxystilbene-2-O-β- D-glucopyranoside (THSG), emodin, and physcion.

In conclusion, we confirmed the superior antiinflammatory effects of K1 to C1 in LPS-activated BV2 cells and demonstrated that the related mechanisms involved suppression of the production of inflammatory mediators and cytokines by blocking the NF-κB and MAPK signaling pathways. Therefore, K1 is expected to be more effective than C1 and can be applied more widely in the development of preventive and therapeutic agents for various inflammation-mediated neurodegenerative diseases.

Author contributions
Conceived and designed the experiments: TWO, YMK Performed the experiments: TWO, YJB. Analyzed the data: TWO, YJB, YMK. Wrote the paper and reviewed the literature: TWO, YMK. All authors have read and agreed to the published version of the manuscript.

Availability of data and materials
All data is available in the main text.

Declarations

Ethics approval and consent to participate
Not applicable.

Consent for publication
Not applicable.

Competing interests
The authors declare that they have no competing interests.

References
1. Kwon HS, Koh SH (2020) Neuroinflammation in neurodegenerative disorders: the roles of microglia and astrocytes. Transl Neurodegener. https://doi.org/10.1186/s40035-020-00221-2
2. Do MH, Kim M, Choi SY, Lee P, Kim Y, Hur J (2021) Wild radish (*Raphanus sativus* var. hortensis f. raphanistroides) root extract protects neuronal cells by inhibiting microglial activation. Appl Biol Chem. https://doi.org/10.1186/s13765-021-00604-7
3. Li QY, Barres BA (2018) Microglia and macrophages in brain homeostasis and disease. Nat Rev Immunol 18(4):225–242. https://doi.org/10.1038/nri.2017.125
4. Tang P, Liu ST, Zhang JS, Ai ZY, Hu Y, Cui LL et al (2024) Ginsenosides as dietary supplements with immunomodulatory effects: a review. Appl Biol Chem. https://doi.org/10.1186/s13765-024-00881-y
5. Nandi A, Counts N, Chen S, Seligman B, Tortorice D, Vigo D et al (2022) Global and regional projections of the economic burden of Alzheimer's disease and related dementias from 2019 to 2050: a value of statistical

life approach. Eclinicalmedicine. https://doi.org/10.1016/j.eclinm.2022.101580

6. Huang HP, Wang J, Huang LQ, Gao SL, Huang P, Wang DL (2014) Germplasm preservation in vitro of polygonum multiflorum thunb. Pharmacogn Mag 10(38):179–184. https://doi.org/10.4103/0973-1296.131032

7. Li M, Yang QD, Du XP (2002) The protection of polygonum multiflorum thunb to the rats' cerebral AChE neurons damaged by kainic acid. J Alzheimers Dis 4(1):60

8. Kang Y, Lee K, Choi J, Komakech R, Min J, Ju S et al (2018) Maximizing seedling and root tuber production in for use in ethnomedicine. S Afr J Bot 119:119–131. https://doi.org/10.1016/j.sajb.2018.08.016

9. Kim DU, Chung JY, Jin SC, Kim MH, Komakech R, Shim KS et al (2020) Effects of processed with KIOM patent on bone remodeling-related protein expression in human osteoblast-like SaOS-2 cells. Evid-Based Compl Alt. https://doi.org/10.1155/2020/4168535

10. Gu DL, Wang Y, Jin HY, Kang S, Liu Y, Zan K et al (2022) Changes of physicochemical properties and immunomodulatory activity of polysaccharides during processing of thunb. Front Pharmacol. https://doi.org/10.3389/fphar.2022.934710

11. Yong-Goo K, Se Jin L, Han Sol K, Ji Hye L, Yuseong C, Youngmin K (2020) Comparison of active compounds for each supplement after processing methods of KIOM <i>polygonum multiflorum</i> thunberg using various ingredient(s). J Agric Life Sci 54(5):37–44

12. Russo MV, McGavern DB (2016) Inflammatory neuroprotection following traumatic brain injury. Science 353(6301):783–785. https://doi.org/10.1126/science.aaf6260

13. Lull ME, Block ML (2010) Microglial activation and chronic neurodegeneration. Neurotherapeutics 7(4):354–365. https://doi.org/10.1016/j.nurt.2010.05.014

14. Kuse Y, Ohuchi K, Nakamura S, Hara H, Shimazawa M (2018) Microglia increases the proliferation of retinal precursor cells during postnatal development. Mol Vis 24:536–545

15. González H, Elgueta D, Montoya A, Pacheco R (2014) Neuroimmune regulation of microglial activity involved in neuroinflammation and neurodegenerative diseases. J Neuroimmunol 274(1–2):1–13. https://doi.org/10.1016/j.jneuroim.2014.07.012

16. Shen ZW, Yang XY, Lan YL, Chen G (2024) The neuro-inflammatory microenvironment: an important regulator of stem cell survival in Alzheimer's disease. J Alzheimers Dis 98(3):741–754. https://doi.org/10.3233/Jad-231159

17. Wang W, Huang FR, Jiang WF, Wang WW, Xiang J (2020) Brilliant blue G attenuates neuro-inflammation via regulating MAPKs and NF-κB signaling pathways in lipopolysaccharide-induced BV2 microglia cells. Exp Ther Med. https://doi.org/10.3892/etm.2020.9244

18. Rivest S (2003) Molecular insights on the cerebral innate immune system. Brain Behav Immun 17(1):13–19. https://doi.org/10.1016/S0889-1591(02)00055-7

19. Jasprica I, Bojic M, Mornar A, Besic E, Bucan K, Medic-Saric M (2007) Evaluation of antioxidative activity of Croatian propolis samples using DPPH[•] and ABTS^{•+} stable free radical assays. Molecules 12(5):1006–1021. https://doi.org/10.3390/12051006

20. Hong KH, Jung J, Kim M, Um MY (2024) Hyperoside ameliorates depression-like behavior in ovariectomized mice. Appl Biol Chem. https://doi.org/10.1186/s13765-024-00897-4

21. Kourosh-Arami M, Hosseini N, Mohsenzadegan M, Komaki A, Joghataei MT (2020) Neurophysiologic implications of neuronal nitric oxide synthase. Rev Neurosci 31(6):617–636. https://doi.org/10.1515/revneuro-2019-0111

22. Jiang Z, Li C, Arrick DM, Yang S, Baluna AE, Sun H (2014) Role of nitric oxide synthases in early blood-brain barrier disruption following transient focal cerebral ischemia. PLoS ONE. https://doi.org/10.1371/journal.pone.0093134

23. Liñares D, Taconis M, Maña P, Correcha M, Fordham S, Staykova M et al (2006) Neuronal nitric oxide synthase plays a key role in CNS demyelination. J Neurosci 26(49):12672–12681. https://doi.org/10.1523/Jneurosci.0294-06.2006

24. Gilroy DW, Lawrence T, Perretti M, Rossi AG (2004) Inflammatory resolution: new opportunities for drug discovery. Nat Rev Drug Discov 3(5):401–416. https://doi.org/10.1038/nrd1383

25. Lawrence T, Willoughby DA, Gilroy DW (2002) Anti-inflammatory lipid mediators and insights into the resolution of inflammation. Nat Rev Immunol 2(10):787–795. https://doi.org/10.1038/nri915

26. Wagner N, Reinehr S, Palmhof M, Schuschel D, Tsai T, Sommer E et al (2022) Microglia activation in retinal ischemia triggers cytokine and toll-like receptor response. J Mol Neurosci 72(1):170. https://doi.org/10.1007/s12031-021-01927-2

27. Wagner N, Reinehr S, Palmhof M, Schuschel D, Tsai TR, Sommer E et al (2021) Microglia activation in retinal ischemia triggers cytokine and toll-like receptor response. J Mol Neurosci 71(3):527–544. https://doi.org/10.1007/s12031-020-01674-w

28. Kyriakis JM, Avruch J (2012) Mammalian mapk signal transduction pathways activated by stress and inflammation: a 10-year update. Physiol Rev 92(2):689–737. https://doi.org/10.1152/physrev.00028.2011

29. Liu YS, Shepherd EG, Nelin LD (2007) MAPK phosphatases—regulating the immune response. Nat Rev Immunol 7(3):202–212. https://doi.org/10.1038/nri2035

30. Leszek J, Barreto GE, Gasiorowski K, Koutsouraki E, Avila-Rodrigues M, Aliev G (2016) Inflammatory mechanisms and oxidative stress as key factors responsible for progression of neurodegeneration: role of brain innate immune system. CNS Neurol Disord Drug Targets 15(3):329–336. https://doi.org/10.2174/1871527315666160202125914

31. Han IO, Kim HS, Kim HC, Joe EH, Kim WK (2003) Synergistic expression of inducible nitric oxide synthase by phorbol ester and interferon-γ is mediated through NF-κB and ERK in microglial cells. J Neurosci Res 73(5):659–666. https://doi.org/10.1002/jnr.10706

32. Jiang CY, Qin XY, Yuan MM, Lu GJ, Cheng Y (2018) 2,3,5,4′-Tetrahydroxystilbene-2-O-beta-D-glucoside reverses stress-induced depression via inflammatory an oxidative stress pathways. Oxid Med Cell Longev. https://doi.org/10.1155/2018/9501427

33. Lee SY, Ahn SM, Wang ZY, Choi YW, Shin HK, Choi BT (2017) Neuroprotective effects of 2,3,5,4′-tetrahydoxystilbene-2-O-β-D-glucoside from against glutamate -induced oxidative toxicity in HT22 cells. J Ethnopharmacol 195:64–70. https://doi.org/10.1016/j.jep.2016.12.001

34. Li ZP, Bi H, Jiang HB, Song JJ, Meng QF, Zhang YZ et al (2021) Neuroprotective effect of emodin against Alzheimer's disease via Nrf2 signaling in U251 cells and APP/PS1 mice. Mol Med Rep. https://doi.org/10.3892/mmr.2020.11747

Publisher's Note